1.5 W green light generation by single-pass second harmonic generation of a single-frequency tapered diode laser

Ole Bjarlin Jensen[1,*], Peter E. Andersen[1], Bernd Sumpf[2], Karl-Heinz Hasler[2], Götz Erbert[2], and Paul Michael Petersen[1]

[1]DTU Fotonik, Department of Photonics Engineering, Technical University of Denmark, Frederiksborgvej 399,DK-4000 Roskilde, Denmark

[2]Ferdinand-Braun-Institut für Höchstfrequenztechnik, Gustav-Kirchhoff- Strasse 4, 12489 Berlin, Germany

**Corresponding author: ojen@fotonik.dtu.dk*

Abstract: More than 1.5 W of green light at 531 nm is generated by single-pass second harmonic generation in periodically poled MgO:$LiNbO_3$. The pump laser is a high power tapered laser with a distributed Bragg reflector etched in the ridge section of the laser to provide wavelength selectivity. The output power of the single-frequency tapered laser is 9.3 W in continuous wave operation. A conversion efficiency of 18.5 % was achieved in the experiments.

©2009 Optical Society of America

OCIS codes: (140.2020) Diode Lasers; (140.3515) Lasers, frequency doubled (190.2620) Harmonic generation and mixing.

References and links

1. L. McDonagh and R. Wallenstein, "Low-noise 62 W CW intracavity-doubled TEM_{00} Nd:YVO_4 green laser pumped at 888 nm," Opt. Lett. **32**, 802-804, (2007).
2. S. V. Tovstong, S. Kurimura, and K. Kitamura, "High power continuous-wave green light generation by quasiphase matching in Mg stoichiometric lithium tantalate," Appl. Phys. Lett. **90**, 051115, (2007).
3. H. K. Nguyen, M. H. Hu, N. Nishiyama, N. J. Visovsky, Y. Li, K. Song, X. Liu, J. Gollier, L. C. Hughes, R. Bhat, and C.-E. Zah, "107-mW low-noise green-light emission by frequency doubling of a reliable 1060 nm DFB semiconductor laser diode," IEEE Photon. Technol. Lett. **18**, 682-684, (2006).
4. M. Iwai, T. Yoshino, S. Yamaguchi, M. Imaeda, N. Pavel, I. Shoji, and T. Taira, "High-power blue generation from a periodically poled MgO:$LiNbO_3$ ridge-type waveguide by frequency doubling of a diode end-pumped Nd:$Y_3Al_5O_{12}$ laser," Appl. Phys. Lett. **83**, 3659-3661, (2003).
5. K. Sakai, Y. Koyata, and Y. Hirano, "Planar-waveguide quasi-phase-matched second-harmonic-generation device in Y-cut MgO-doped $LiNbO_3$," Opt. Lett. **31**, 3134-3136, (2006).
6. K. Sakai, Y. Koyata, N. Shimada, K. Shibata, Y. Hanamaki, S. Itakura, T. Yagi, and Y. Hirano, "Master-oscillator power-amplifier scheme for efficient green-light generation in a planar MgO:PPLN waveguide," Opt. Lett. **33**, 431-433, (2008).
7. M. Maiwald, S. Schwertfeger, R. Güther, B. Sumpf, K. Paschke, C. Dzionk, G. Erbert, and G. Tränkle, "600 mW optical output power at 488 nm by use of a high-power hybrid laser diode system and a periodically poled MgO:$LiNbO_3$ bulk crystal," Opt. Lett. **31**, 802-804, (2006).
8. M. Chi, O. B. Jensen, J. Holm, C. Pedersen, P. E. Andersen, G. Erbert, B. Sumpf, and P. M. Petersen, "Tunable high-power narrow-linewidth semiconductor laser based on an external-cavity tapered amplifier," Opt. Express **13**, 10589-10596 (2005).
9. R. Parke, D. F. Welch, A. Hardy, R. Lang, D. Mehuys, S. O'Brien, K. Dzurko, and D. Scifres, "2.0 W CW, diffraction-limited operation of a monolithically integrated master oscillator power amplifier," IEEE Photon. Technol. Lett. **5**, 297-300, (1993).
10. M. Uebernickel, C. Fiebig, G. Blume, K. Paschke, B. Eppich, R. Güther, and G. Erbert, „400 mW and 16.5% wavelength conversion efficiency at 488 nm using a diode laser and a PPLN crystal in single-pass configuration," Appl. Phys. B **93**, 823-827, (2008).
11. K. Paschke, J. Behrendt, M. Maiwald, J. Fricke, H. Wenzel, and G. Erbert, "High-power, single mode 980 nm DBR tapered diode lasers with integrated 6^{th} order surface gratings based on simplified fabrication process," Proc. SPIE **6184**, 618401, (2006).

12. A. Knauer, G. Erbert, R. Staske, B. Sumpf, H. Wenzel, and M. Weyers, "High-power 808-nm lasers with a super-large optical cavity," Semicond. Sci. Technol. **20**, 621–624 (2005).
13. G. D. Boyd and D. A. Kleinman, "Parametric Interaction of Focused Gaussian Light Beams," J. Appl. Phys. **39**, 3597-3639 (1968).
14. G. Blume, M. Uebernickel, C. Fiebig, K. Paschke, A. Ginola, B. Eppich, R. Güther, and G. Erbert, "Rayleigh length dependent SHG conversion at 488nm using a monolithic DBR tapered diode laser," Proc. SPIE **6875**, 68751C-1-12, (2008).
15. M. M. Fejer, G. A. Magel, D. H. Jundt, and R. L. Byer," Quasi-Phase-Matched Second Harmonic Generation: Tuning and Tolerances," IEEE J. Quantum Electron. **28**, 2631-2654 (1992).
16. D. E. Zelmon, D. L. Small, and D. Jundt, "Infrared corrected Sellmeier coefficients for congruently grown lithium niobate and 5 mol. % magnesium oxide-doped lithium niobate," J. Opt. Soc. Am. B **14**, 3319-3322, (1997).
17. G. J. Edwards and M. Lawrence, "A temperature-dependent dispersion equation for congruently grown lithium niobate," Opt. Quantum Electron. **16**, 373-374, (1984).
18. Y. S. Kim and R. T. Smith, "Thermal expansion of lithium tantalate and lithium niobate single crystals," J. Appl. Phys. **40**, 4637-4641 (1969).

1. Introduction

Many applications within biomedicine, material processing and displays require light sources in the visible region. In particular display applications require compact and efficient red, green and blue light sources with high beam quality. The red spectral region is covered by direct emission from diode lasers and the blue region will be covered by nitride-based diode lasers. The green spectral region, however, is not easily accessible by direct diode lasers.

Several methods exist for generation of green light. The most well-known is probably second harmonic generation (SHG) of the output from diode pumped solid state or fiber lasers. Here many Watts of green light can be generated and with very good spectral and spatial quality [1,2]. Solid state lasers have the disadvantage that the output needs modulation through the use of for instance acousto-optic modulators because of the long carrier lifetime in solid state laser materials. This can be overcome by the use of diode lasers as the pump source for the SHG as the diode lasers can be modulated directly, at the expense of output power, though. Different approaches have been used to generate green light by SHG of diode lasers. One of the most promising solutions for low power green light generation is the use of nonlinear waveguides for SHG of a distributed feedback (DFB) or distributed Bragg reflector (DBR) laser [3]. The waveguide offers very high conversion efficiency as the light is tightly confined in the waveguide. Unfortunately, waveguides have shown power handling problems for green powers above a few hundred milliwatts [4]. Recently, it has been demonstrated that higher power can be achieved by the use of planar waveguides, where the light is only confined in one direction. An output power of 1.08 W at a conversion efficiency of 30 % has been reached by the use of a fiber laser as the pump source [5] and 346 mW output power at an internal conversion efficiency of 38 % was achieved when a master-oscillator-power-amplifier (MOPA) was used [6]. However the coupling of the astigmatic and elliptical output from the MOPA into the waveguide is not trivial and only a coupling efficiency of about 20 % was achieved reducing the overall conversion efficiency to 7.6 %. A MOPA configuration has also been used to generate 600 mW of 488 nm light by SHG in periodically poled $MgO:LiNbO_3$ (PPMgLN) with a conversion efficiency of 15 % [7].

Tapered diode lasers with good spectral and spatial quality has recently become available as efficient pump sources for SHG. Different approaches for achieving good spectral quality including external cavity approaches [8] and DBR tapered lasers [9] have proven successful and these methods significantly reduce the size and complexity of the pump laser compared to MOPA configurations. 400 mW of light at 488 nm has been generated by single-pass SHG of a DBR tapered laser in PPMgLN with a conversion efficiency of 16.5% [10].

In this work we developed a novel DBR tapered diode laser as pump source for the SHG process. The DBR tapered laser outputs more than 9 W of nearly diffraction limited power in a narrow spectral region. The laser is frequency doubled in a single-pass configuration using a

bulk periodically poled MgO:$LiNbO_3$ (PPMgLN) crystal and we obtain 1.58 W of output power at a wavelength of 531 nm corresponding to a conversion efficiency from infrared to green of 18.5%. The results represent the highest single-pass SHG green output power using a diode laser as pump source.

2. The DBR tapered laser

The laser source shown in Fig. 1 consists of a 6 mm long DBR tapered diode laser with a sixth order surface grating similar to the one reported in Ref. 11. The ridge waveguide of the tapered diode laser is 2 mm long and consists of a 1 mm long unpumped DBR section and a 1 mm long pumped ridge waveguide section. The tapered section is 4 mm long with a taper angle of 6°. The ridge and the tapered section of the laser have separate contacts so that the currents to both sections can be controlled individually. The laser structure is made using a super large optical cavity (SLOC) [12] and the divergence of the beam in the vertical direction is 15° (FWHM). The laser is mounted p-side up on a CuW heat spreader which is again mounted on a 25 x 25 mm footprint heat sink for efficient cooling of the laser.

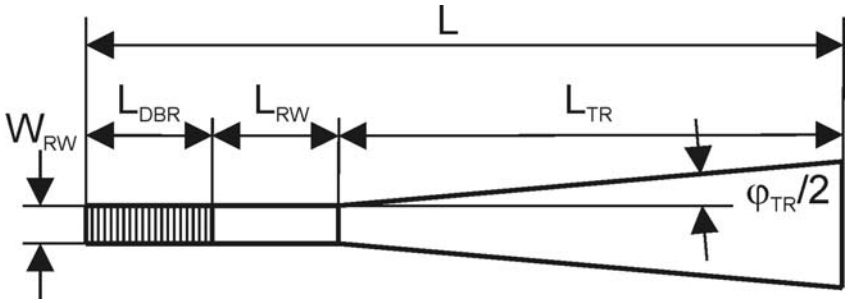

Fig. 1. Sketch of the DBR tapered laser.

The laser emits an output power of more than 9 W at a ridge section current of 300 mA and a taper section current of 14 A. The laser output power is dependent on the laser temperature as shown in Fig. 2, where output power characteristics are shown for two different operating temperatures. The difference in output power is very small for the 5ºC temperature difference and it is also noticed that the output power shows no signs of roll-over even at 9 W.

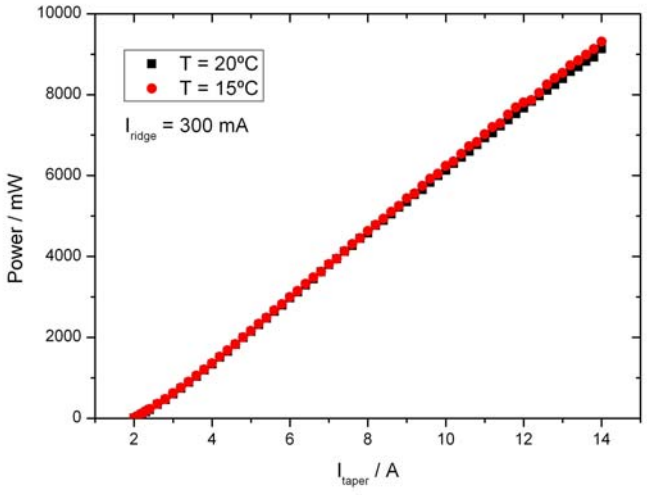

Fig. 2. Output power from the DBR tapered laser vs. current to the taper section at 300 mA ridge section current at operating temperatures of 15ºC (red dots) and 20ºC (black squares).

The wavelength of the laser is dependent on the current to the ridge section, the current to the taper section and the temperature of the laser. In Fig. 3 we show the dependence of the laser wavelength on the taper section current at two different laser temperatures and the laser wavelength dependency on the laser temperature. The dependence of the laser wavelength on the taper current above 5 A is approximately linear with a change in wavelength of 0.023 nm/A. The wavelength change with temperature is also approximately linear with a slope of 0.087 nm/ºC between the occasional mode hops evident in Fig. 3.

The beam propagation parameter, M^2 ($1/e^2$), of the laser in the slow axis is below 1.3 at all power levels and approximately 70 % of the power is contained within the main lobe of the output beam at 9 W of output power.

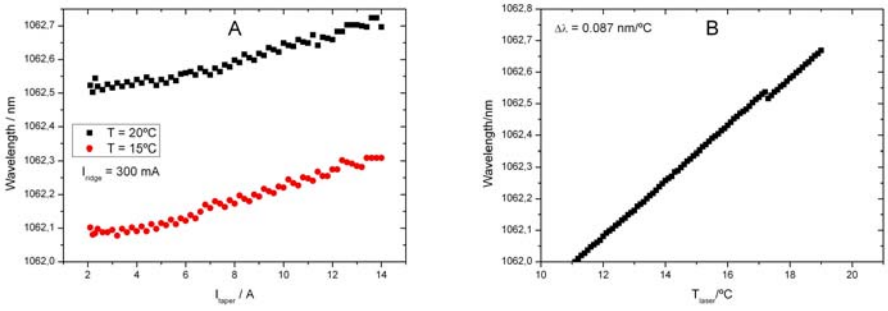

Fig. 3. (A) The emitted laser wavelength vs. taper section current at a ridge section current of 300 mA and laser temperatures of 15ºC and 20ºC. (B) The laser wavelength vs. temperature at a fixed ridge section current of 300 mA and a taper section current of 14 A.

The spectrum of the laser is shown in Fig. 4 at 14 A taper section current and 300 mA ridge current at a laser temperature of 14.3ºC. This temperature is used, as the obtained wavelength of 1062.3 nm facilitated phase matching in the SHG process. The spectrum is measured with an Advantest Q8347 optical spectrum analyzer. The laser emits light in a

single longitudinal mode with a spectral width that is resolution limited to 0.006 nm. The side mode suppression is above 25 dB limited by the dynamic range of the optical spectrum analyzer.

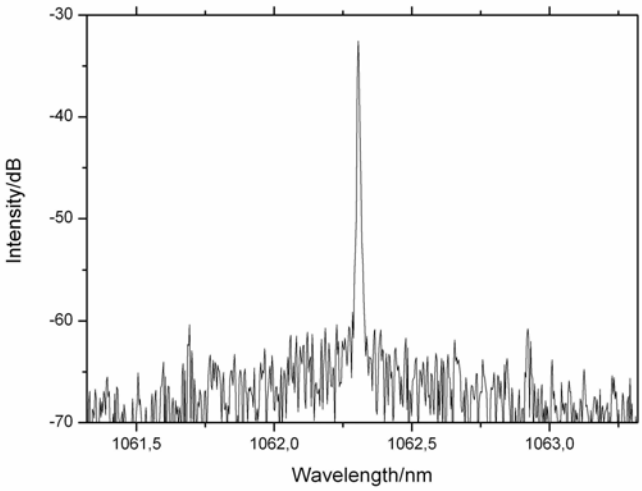

Fig. 4. Spectrum of the DBR tapered laser at a taper section current of 14 A and 300 mA ridge section current. The laser temperature was 14.3ºC.

3. SHG experiments

The experimental setup for SHG is shown in Fig. 5. The output from the DBR tapered diode laser is collimated in the fast axis using an aspherical lens with a focal length of 3.1 mm and a numerical aperture of 0.68. Due to the astigmatism of tapered diode lasers, an additional cylindrical lens with a focal length of 15 mm is used to collimate the beam in the slow axis and to generate an approximately circular beam. The beam is passed through a half-wave plate and an optical isolator in order to avoid feedback to the tapered diode laser and to be able to adjust the power level to the SHG crystal without changing the laser current, which will change the astigmatism and wavelength of the laser, thus reducing the SHG efficiency. A second half-wave plate is used after the isolator to correct the polarization of the beam to fit with the optimal polarization for SHG. A folding mirror and a focusing lens with a focal length of 100 mm are used to generate a beam waist in the nonlinear crystal with a radius of approximately 60 μm. This beam waist radius is significantly larger than 29 μm, which is predicted to be optimum according to the theory of Boyd and Kleinman [13] but proved to be optimum in the experiments. This may be explained by the non-Gaussian beam profile of the tapered laser [14]. A filter is used to separate the fundamental laser light from the generated green light.

The nonlinear crystal used in these experiments is a 2 x 0.5 x 30 mm (width x height x length) PPMgLN crystal (HCPhotonics). The crystal is poled with a single period of 6.92 μm. The crystal is cut with an angle of 10° in the width direction at both ends and antireflection coated at both 1064 nm and 532 nm to avoid feedback from the crystal facets. The crystal is temperature stabilized using an oven in order to achieve phase matching at the laser wavelength. In the experiments the crystal temperature was 35°C.

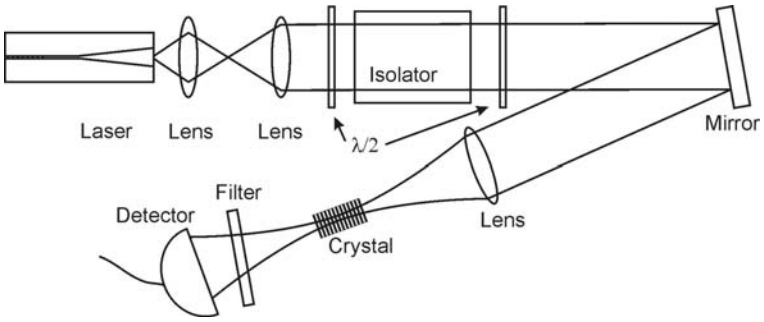

Fig. 5. Sketch of the experimental setup for single-pass SHG of a DBR tapered laser.

For optimum phase matching of the laser wavelength and the PPMgLN temperature, the laser temperature was set at 14.3°C where the laser wavelength is 1062.3 nm. After the beam has passed through the isolator, waveplates and lenses, 8.52 W is available before the PPMgLN crystal. The SHG output power reached a maximum of 1.58 W and the SHG power characteristics are shown in Fig. 6. Here the experimental results are fitted to the theoretical curve for second harmonic generation with pump depletion following the relation

$$P_{SHG} = P_{laser} \tanh^2(\sqrt{\eta_{SHG} P_{laser}}) \quad (1)$$

Here η_{SHG} is the nonlinear conversion efficiency. The fit gives a nonlinear conversion efficiency of η_{SHG} = 2.5 %/W in the experiments. The power conversion efficiency in the SHG experiment is 18.5 % and the wall-plug efficiency is approximately 5 %.

The beam quality of the SHG beam is close to the diffraction limit with a beam quality of $M^2 < 1.3$ ($1/e^2$).

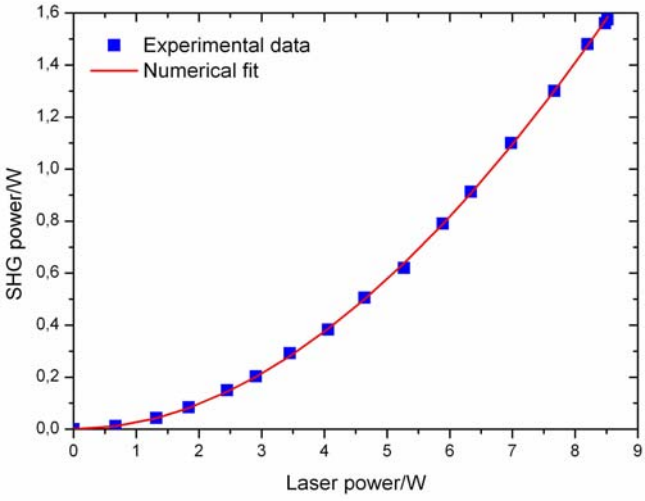

Fig. 6. SHG output power vs. fundamental input power. The red line is a numerical fit using the depleted pump approximation resulting in a nonlinear conversion efficiency of 2.5 %/W.

The temperature and wavelength acceptance bandwidths have been measured by changing the crystal temperature and laser temperature, respectively. The resulting phase matching curves are shown in Fig. 7 at 1 W of input power and at 8.52 W of input power, respectively. The temperature acceptance bandwidth for the PPMgLN crystal is 0.9 °C and the wavelength acceptance bandwidth is 0.075 nm at low input power. The bandwidths increase

for high input power to 1.1ºC and 0.09 nm for the temperature and wavelength respectively. The increase in bandwidths at high input power is believed to be caused by heating of the crystal by absorption of both the fundamental beam and the SHG beam. The acceptance bandwidths can be calculated using [15]

$$\Delta T_{FWHM} = \frac{0.4429\,\lambda}{L}\left|\frac{\partial \Delta n}{\partial T} - \alpha \Delta n\right|^{-1} \tag{2}$$

for the temperature acceptance bandwidth and

$$\Delta \lambda_{FWHM} = \frac{0.4429\,\lambda}{L}\left|\frac{n_2 - n_1}{\lambda} + \frac{\partial n_1}{\partial \lambda} - \frac{\partial n_2}{2\partial \lambda}\right|^{-1} \tag{3}$$

for the wavelength acceptance bandwidth respectively. Here λ is the laser wavelength, L is the crystal length, n is the refractive index and α is the coefficient of linear thermal expansion. Using the Sellmeier equations [16], its derivatives [17] and the thermal expansion coefficient [18] for MgO:$LiNbO_3$ we find that the measured results at low input power indicate an effective length of our crystal of 27 mm.

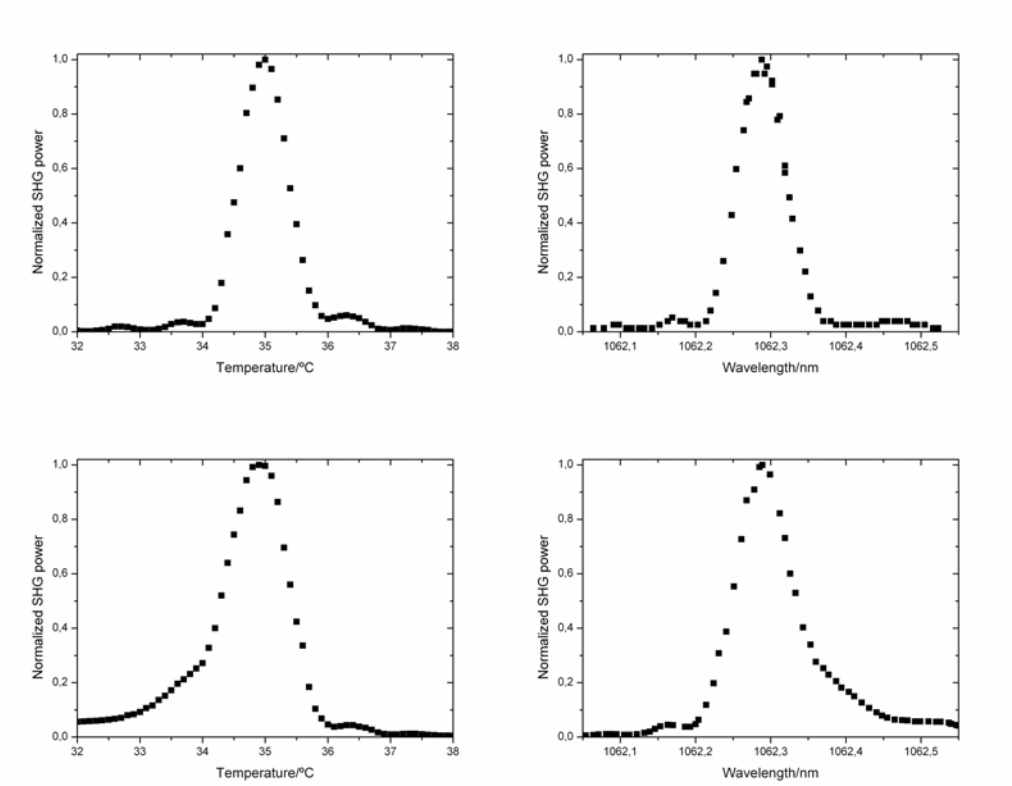

Fig. 7. Measured temperature (left) and wavelength (right) tuning curves for the PPMgLN crystal at 1 W input power (top) and at 8.52 W input power (bottom).

The power stability of the green light was measured for a period of 1 hour at a green output power of 1.5 W. The output power was 1.5 W ± 0.04 W corresponding to a variation of ± 3 %. In the measurement no precautions have been taken to minimize temperature fluctuations caused by air flow and all components were placed separately on an optical table. The measured green output power is shown in Fig. 8. We find no indication of power handling problems for the PPMgLN crystal.

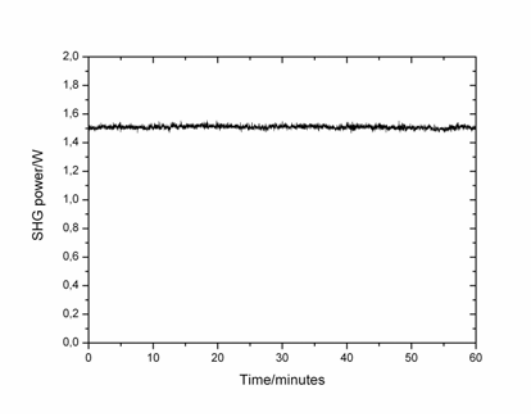

Fig. 8. Measured green output power for a period of 1 hour.

4. Conclusion

In conclusion we have used a distributed Bragg reflector tapered diode laser with an output power of more than 9 W as the pump source for second harmonic generation. By employing single-pass second harmonic generation in a bulk PPMgLN crystal we generate 1.58 W of green light at a wavelength of 531 nm resulting in 18.5 % conversion efficiency from infrared light to green light. To our knowledge, this represents the highest green power obtained by single-pass SHG of a diode laser source.

Acknowledgements

This project was supported by the EU-FP6 integrated project WWW.BRIGHTER.EU contract IST-2005-035266.